Colloid Polym Sci 277:777–784 (1999)

ORIGINAL CONTRIBUTION

A. Hieke
H.-D. Dörfler

Selected X-ray diffraction and differential scanning calorimetry measurements on nonaqueous liquid crystals and gel phases in the K-myristinate/glycerol binary system

Received: 3 March 1999
Accepted in revised form: 29 March 1999

Dedicated to Professor Dr. Dr. h.c. G. Lagaly on occasion of his 60th Birthday

A. Hieke · H.-D. Dörfler (✉)
TU Dresden, Institut für Physikalische Chemie und Elektrochemie
Kolloidchemie, Mommsenstrasse 13
D-01062, Dresden, Germany

Abstract Samples from the three selected concentrations $x_{KC_{14}} = 0.25, 0.37,$ and 0.50 of the K-myristinate/glycerol (KC_{14}/Gl) binary system have been investigated by means of small- and wide-angle X-ray diffraction measurements as well as differential scanning calorimetry (DSC) measurements as a function of temperature. The results are

- The G_1 gel phase, contained in the preliminary phase diagram according to Dörfler and Senst [(1993) *Colloid Polym Sci* 271: 173], is nonexistent.
- The same applies of the isotropic phase in the preliminary phase diagram according to Dörfler and Senst. Initially an isotropic or a cubic phase was assumed based on polarized microscopy texture observations. X-ray diffraction and DSC measurements provided no indication for their existence.
- Due to the nonexistence of the G_1 and isotropic phases the preliminary phase diagram of the KC_{14}/Gl binary system had to be corrected. The region of the lamellar phase extends over a wider region.
- X-ray diffraction and DSC measurements provided concordant results, which were further confirmed by electron microscopic investigation. Differences in phase-transition points from DSC data obtained for rising and falling temperatures have been observed.
- The crystalline-to-gel phase transition correlates with a sharp shift in the *d* value of the first small-angle reflex.
- The gel phase is accompanied by a distinct splitting of the first small-angle reflexes. The wide-angle reflexes show rearrangement and reduced intensity.
- Similar to the crystalline-to-gel phase transition, the gel-to-lamellar phase transition is accompanied by a sharp change in the *d* values.

Key words Lyotropic liquid crystals · X-ray diffraction · Calorimetry · Gel phase · K-myristinate

Introduction

Our previous works reported methodical developments for X-ray diffraction (XRD) measurements and data analysis on lyotropic liquid crystals applied to K-soap/glycerol systems including selected investigations on two samples of the K-laurate/glycerol (KC_{12}/Gl) binary system as a function of temperature [1–3]. In these publications all experimental procedures are described.

This paper continues these investigations with the K-myristinate/Gl (KC_{14}/Gl) binary system. Here, samples with concentrations $x_{KC_{14}} = 0.25, 0.37,$ and 0.50 have been examined. In accordance with Fig. 1a previous polarized microscopy texture observations revealed [3]

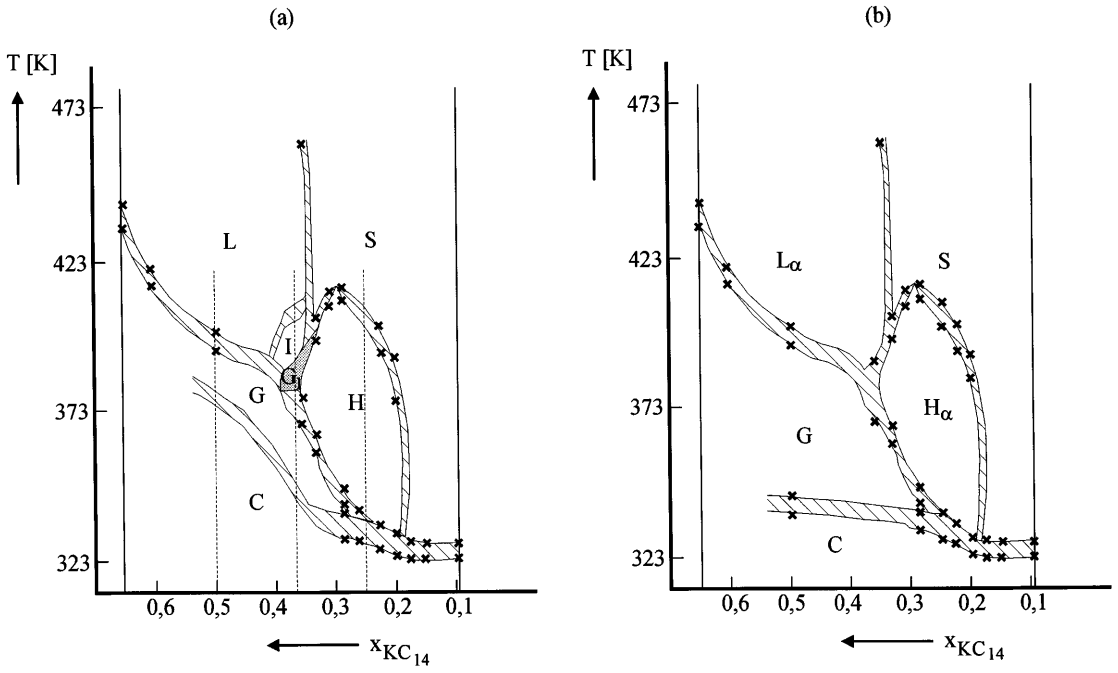

Fig. 1a, b Cutout of the phase diagram of the K-myristinate/glycerol (KC_{14}/Gl) binary system. **a** Preliminary phase diagram on polarized microscopy texture observations according to Ref. [3]. **b** Revised phase diagram according to our X-ray diffraction and differential scanning calorimetry (*DSC*) measurements. C = crystalline phase, G = gel phase, H_α = hexagonal phase, L_α = lamellar phase (chains fluid), S = isotropic, micellar solution, G_1 = second gel phase (nonexistent), I = isotropic phase (nonexistent)

that possibly two different types of gel phases, G and G_1, and an isotropic (I) phase might exist between the regions of the hexagonal (H_α) and lamellar (L_α) phase. The confirmation of their existence was the target of our investigations. Furthermore, measurements on samples with the above-mentioned concentrations in the G, L_α, and H_α phases were intended to provide insight into the structure-creation process beginning with the crystalline (C) phase. The methods are given in Refs. [1, 2].

A representative parameter called the "*d* value" will be used for the discussion of the results from XRD measurements. A brief definition of it with respect to the various phases shall be given. Since the complete determination of the crystallographic parameters in real space is practically impossible for the lyotropic systems considered [2, 4], the available information is limited to some of the reciprocal values depending on the degree of crystallographic order in the phase. With the exemption of the I phase at least one long-spacing periodicity within the structures exists that correlates to the chain length of the soap molecules. In the case of crystalline phases the *d* value is identical to $d_{001} = (c^*)^{-1}$ quantifying the perpendicular distance between 001 planes as illustrated in Fig. 2. It will simply be referred to as the *d* value of the respective small-angle reflexes enabling a direct comparison between different systems and phases. In the crystalline phases only three further reciprocal parameters can be determined with certainty.

The structures investigated significantly lose crystallographic order with the transition to the G phase, mainly within the [*a*, *b*] planes (typical distances of r = 0.2–0.4 nm); however, long-spacing periodicity is still present in the modified appearance of two distinct small-angle reflexes, including higher orders, and their corresponding crystallographic plane distances. The *d* values are identical to those plane distances illustrated in Fig. 3. With the transformation to H_α phases cylindrical structures are formed with the crystallographic parameter *a* as the edge length of the hexagons. The small-angle reflex with the lowest angle corresponds to the perpendicular packaging distance $d_{100} = a \sin(60°)$ of the imagined layers formed by the cylinders and is referred to as the *d* value as also illustrated in Fig. 3. For L_α phases the *d* value describes the distance of the molded [*a*, *b*] planes, the only remaining periodicity of these one-dimensionally ordered systems.

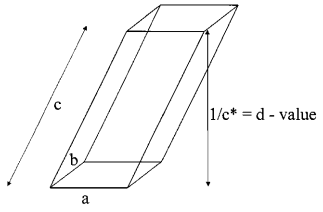

Fig. 2 Definition of the *d* value used for the crystalline phases: $d_{001} = (c^*)^{-1}$, the perpendicular distance between the [*a, b*] planes

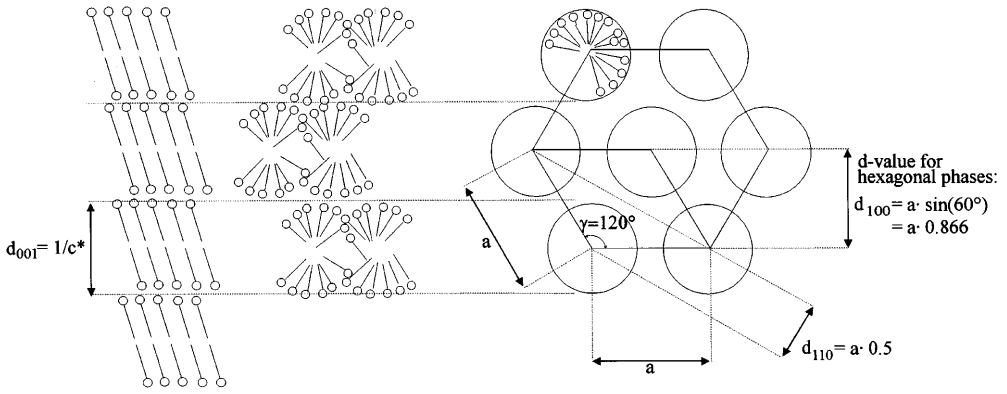

Fig. 3 The transformation from a C to a H_α phase and the definition of the parameter d. C and G phases: $d_{001} = (c^*)^{-1}$, the perpendicular distance between the $[a, b]$ planes; H_α phases: perpendicular packing distance $d_{100} = a \sin(60°)$ of the imagined layers formed by the cylinders

Investigations of the KC_{14}/Gl system with a concentration $x_{KC_{14}} = 0.25$

According to the phase diagram in Fig. 1a the C phase is immediately followed by a H_α phase and the transition is characterized by a broad two-phase region.

Measurement results are shown in Fig. 4, which condenses the wide-angle diffractograms and the DSC data for rising temperature. According to the DSC curve the transition from the C phase to the H_α phase occurs at $T \approx 338$ K. Remarkably, the DSC peak flattens out towards higher temperatures. Comparison with the diffractograms for the temperature range $T \approx 303$–333 K shows that the wide-angle reflexes display only reduced intensity approaching the phase transition; however, the number and the position of the reflexes remain unchanged. It is therefore confirmed that between the C phase and the H_α phase no further G_1 phase exists. As expected, within the two-phase region at $T \approx 338$ K reflexes belonging to the C phase as well as reflexes belonging to the H_α phase can be found.

Small-angle diffractograms for rising temperature steps are shown in Fig. 5. In accordance with the wide-angle diffractograms further confirmation for the $C \leftrightarrow H_\alpha$ phase transition can be found. The distinct d value ratio $1{:}\sqrt{3}{:}\sqrt{4}$ can clearly be detected and furthermore the typical sharp and intense 001 reflex of the H_α

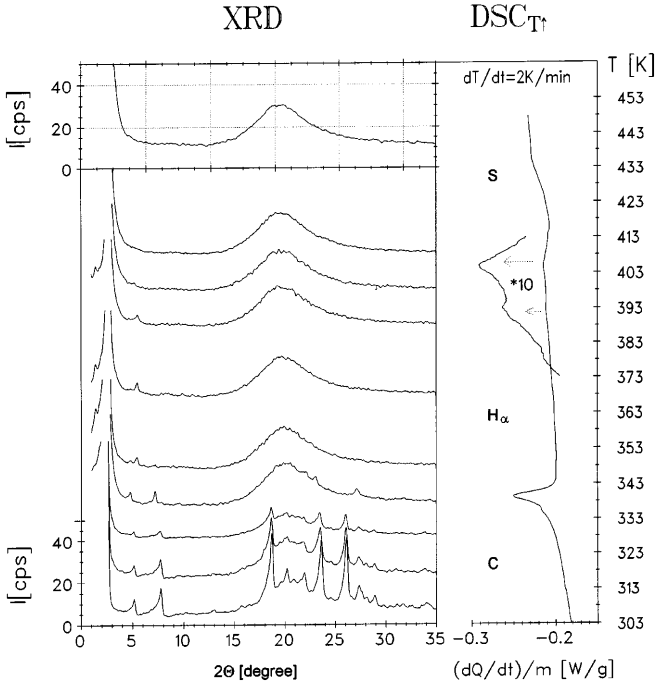

Fig. 4 Comparison of wide-angle X-ray diffractograms with the DSC curve for rising temperature of the KC_{14}/Gl system, $x_{KC_{14}} = 0.25$

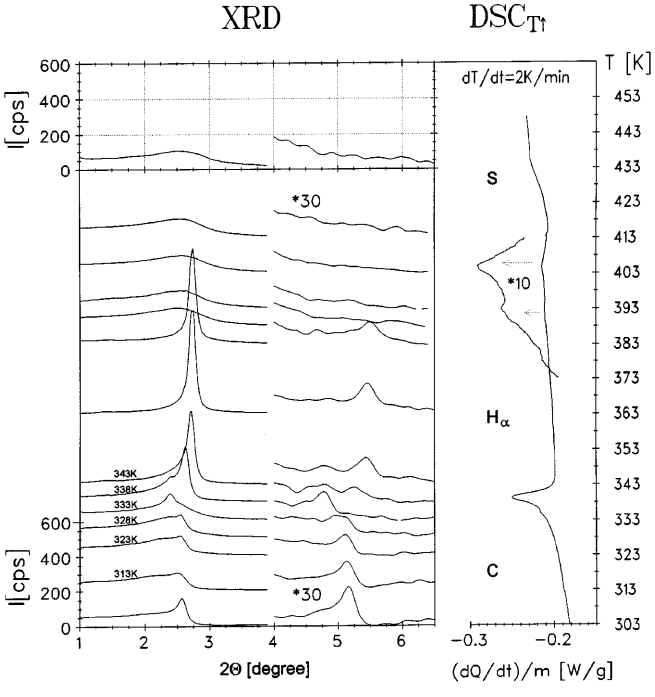

Fig. 5 Small-angle X-ray diffractograms and the DSC curve for rising temperature of the KC_{14}/Gl system, $x_{KC_{14}} = 0.25$

phase appears, usually 3 times the intensity of the 001 reflex of the C phase.

Plotting the d values of the first small-angle XRD reflexes and the DSC data for rising and falling temperatures as illustrated in Fig. 6 shows that the transition to the H_α phase correlates with a sharp shift of the small-angle 001 reflex equivalent to $\Delta d \approx +0.25$ nm. During the transition to the L_α phase the d values reach a minimum. Furthermore, it can be seen that phase transitions can be undercooled by about $\Delta T \approx 10$ K.

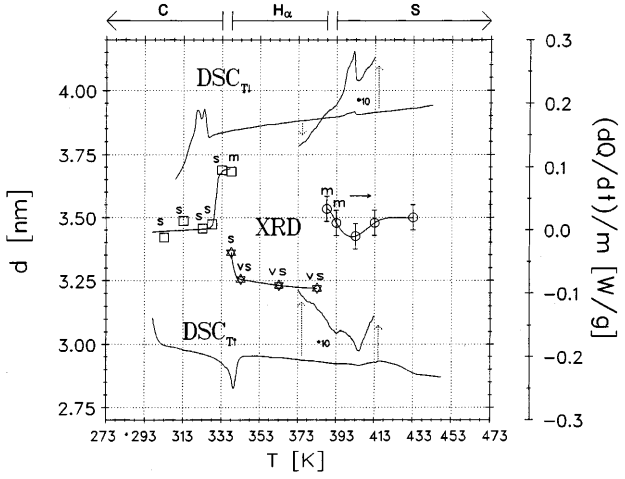

Fig. 6 Comparison of the d values of the first small-angle reflexes with the DSC curve obtained for rising and falling temperatures of the KC_{14}/Gl system, $x_{KC_{14}} = 0.25$. □ reflexes of the C phase; ✡ reflexes of the H_α phase, ○ reflexes of the isotropic phase. Reflex intensity: w = weak, m = medium, s = strong, vs = very strong

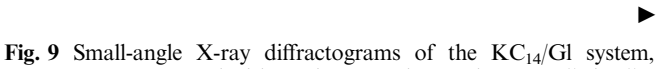

Fig. 9 Small-angle X-ray diffractograms of the KC_{14}/Gl system, $x_{KC_{14}} = 0.37$, measured with a primary and secondary so-called soller collimator and the narrowest possible primary beam guidance (smallest exposed sample core) for T = 388, 393, 398, and 403 K; 72 hours measurement time per diffractogram, data filtered using a Blackman window with $f_c = 100$ ($f_{max} = 209$, $n_{data} = 418$)

Investigations of the KC_{14}/Gl system with a concentration $x_{KC_{14}} = 0.37$

The concentration $x_{KC_{14}} = 0.37$ was chosen to verify if indeed a G_1 phase region exists and if it is really followed by an I phase for rising temperatures. The results of the XRD measurements in the wide-angle range and the DSC data for rising temperature are shown in Fig. 7. According to the DSC curve only two transitions occur. The XRD data allow unambiguous identification of C, G, and L_α phases. The G ↔ L_α phase transition appears in the DSC curve as a peak with two smaller submaxima; however, these do not relate to a phase transition of the presumed G_1 or I phases.

The diffractograms also provide clues to the gradual degradation of the crystalline structure for rising

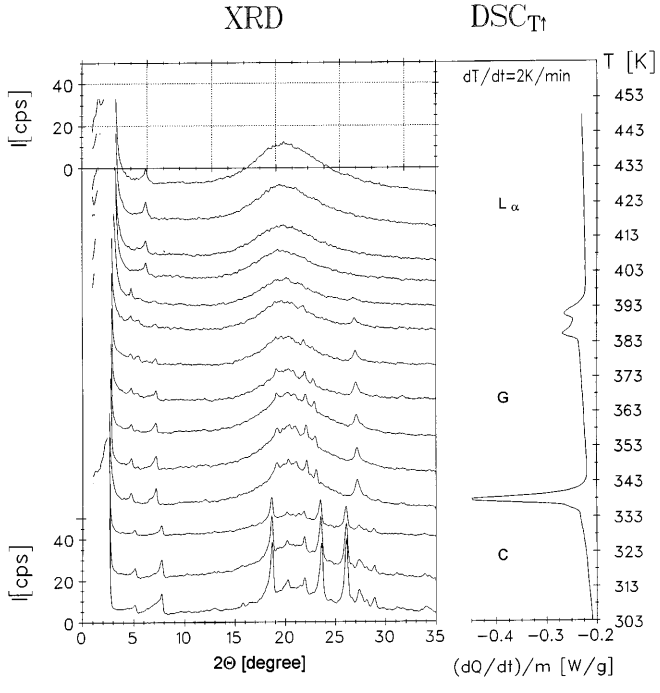

Fig. 7 Comparison of wide-angle X-ray diffractograms with the DSC curve for rising temperature of the KC_{14}/Gl system, $x_{KC_{14}} = 0.37$

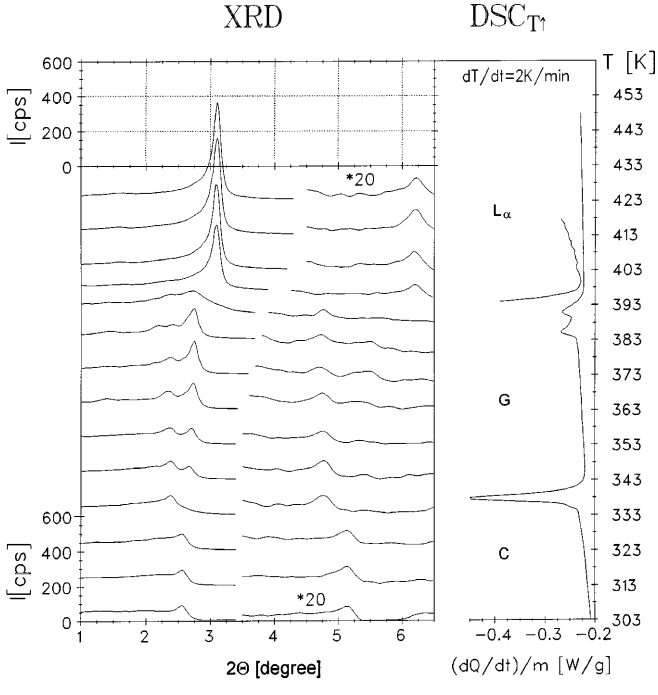

Fig. 8 Small-angle X-ray diffractograms and the DSC curve for rising temperature of the KC_{14}/Gl system, $x_{KC_{14}} = 0.37$

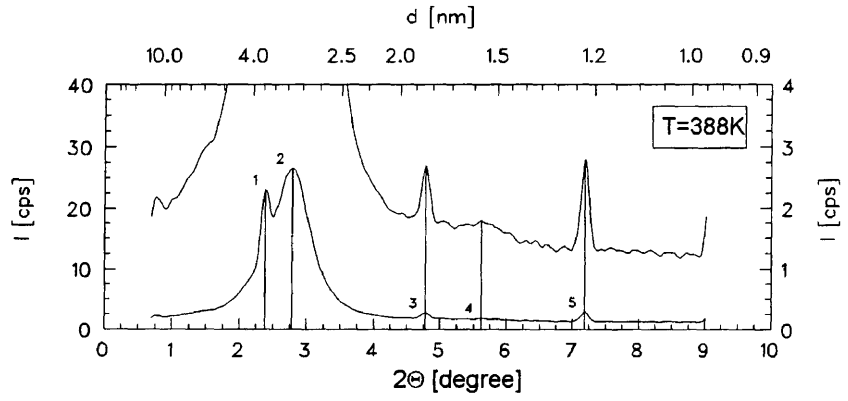

Nr.	2θ[°]	d[nm]	1/d[1/nm]	I[cps]
1	2.380	3.7125	0.2694	23.0
2	2.780	3.1784	0.3146	26.5
3	4.780	1.8489	0.5409	2.7
4	5.620	1.5727	0.6359	1.8
5	7.180	1.2313	0.8121	2.8

WAVELENGTH= .1542 nm

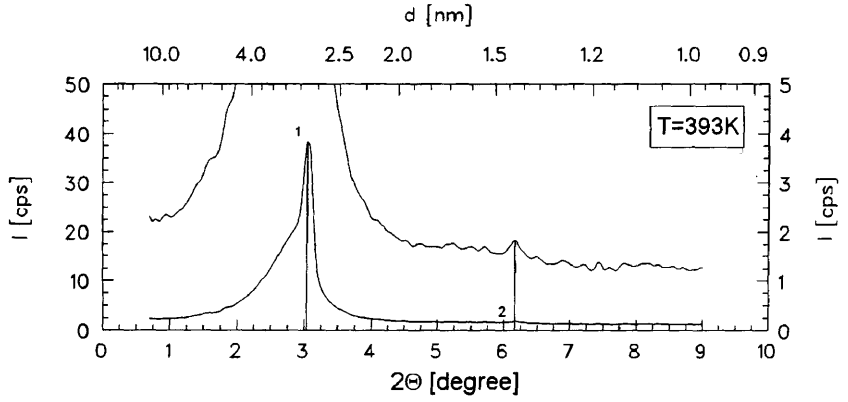

Nr.	2θ[°]	d[nm]	1/d[1/nm]	I[cps]
1	3.040	2.9066	0.3440	38.4
2	6.160	1.4349	0.6969	1.8

WAVELENGTH= .1542 nm

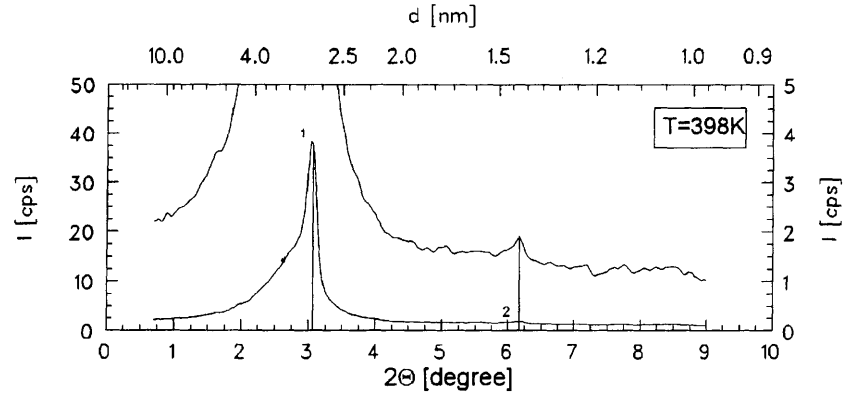

Nr.	2θ[°]	d[nm]	1/d[1/nm]	I[cps]
1	3.060	2.8876	0.3463	37.9
2	6.160	1.4349	0.6969	1.9

WAVELENGTH= .1542 nm

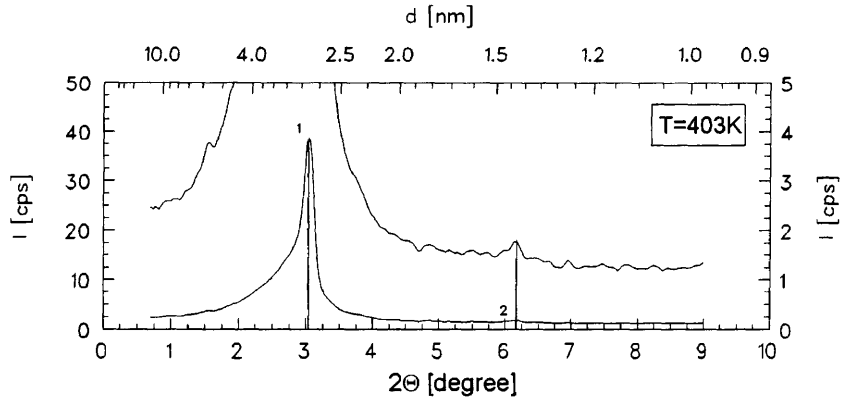

Nr.	2θ[°]	d[nm]	1/d[1/nm]	I[cps]
1	3.040	2.9066	0.3440	38.7
2	6.160	1.4349	0.6969	1.8

WAVELENGTH= .1542 nm

KMG-37

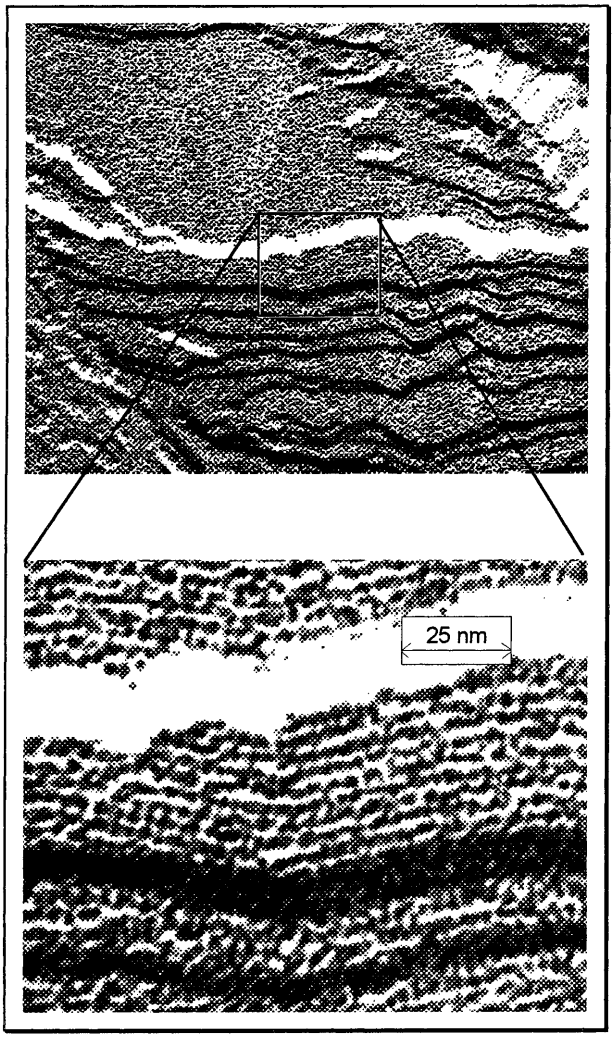

Fig. 10 Transmission electron microscopy (*TEM*) image of a freeze-fracture representation of a sample containing KC_{14}/Gl, $x_{KC_{14}} = 0.37$, at $T = 403$ K within the L_α phase region of the phase diagram

temperature as can be seen between $T = 303$ and 333 K in Fig. 7. The intensity of the diffractograms is reduced, but the reflex number and the position is again maintained. The following region of the G phase between $T = 338$ and 388 K exhibits further intensity-reduced, weaker, and rearranged reflexes which allow a clear distinction between the C and G phases.

Small-angle diffractograms and the DSC curve for rising temperature are shown in Fig. 8. A characteristic sharp shift of the small-angle 001 reflex occurs, equivalent to $\Delta d \approx +0.25$ nm. In addition, the typical splitting of the small-angle reflexes, accompanying the transition in the G phase, can be observed.

In Fig. 9 the small-angle X-ray diffractograms, measured with primary and secondary so-called soller collimators and the narrowest possible primary beam guidance (smallest exposed sample core) for $T = 388$, 393, 398, and 403 K and measurement times per diffractogram of 3 days are shown. The data have been filtered by applying a Blackman window with $f_c = 100$ ($f_{max} = 209$, $n_{data} = 418$) for enhanced noise suppression.

At $T = 388$ K the splitting of the small-angle reflexes, characteristic for the G phase of all observed K-soap/glycerol systems, is still present. A further specific particularity of this system is the very broad second reflex, leading to the d values present in the L_α phase. Nevertheless, it has to be considered as a reflex in terms of diffraction since a second order of it occurs, though this is very weak in intensity. The peak width is significantly reduced with increased perfection of the lamellar structure. The reversal decay of the peaks occurs comparably gradually caused by the reduced but continued presence of a gel-like structure. This can be seen on the elevated left slope of the first peak in the diffractograms 2–4 in Fig. 9.

All the measurements allow the conclusion to be drawn that neither an additional G_1 phase nor an I phase (possibly a cubic phase) in the temperature range considered can be detected by means of XRD.

The same conclusion was reached from the investigation of digitalized video images of polarized microscopy texture observations. These were performed by utilizing an S-VHS video camera/recorder (Panasonic) and a "Screen Machine" (Fast Electronics) video frame grabber installed in an Apple Macintosh computer. By applying several digital image enhancing techniques to the images obtained the potential structures would become more clearly visible or even perceptible at all [4]. The decomposition of the G phase and the successive creation of the L_α phase was evidently observable; however, a completely textureless image never appeared as would have been characteristic for an I or cubic phase.

Furthermore it was attempted to obtain transmission electron microscope images of freeze-fraction samples at $x_{KC_{14}} = 0.37$ and $T = 403$ K as shown in Figs. 10 and 11 displaying the scanned and dynamically contrasted enhanced images. The results may be interpreted as already described.

In Fig. 10 lamellar portions of the structure are clearly recognizable; however, the closeup shows that these lamellas posses only a reduced order. Beside the lamellar layers areas with what can be called "short-range bent" structural parts were found: these are shown in Fig. 11 and especially the closeup reveals that the surface normals of these bent structures face all directions. They may be imagined as very small disordered lamellas of arbitrary orientation. These findings are in accordance with the interpretation of the diffractograms. Therefore, the singular G_1 phase (see Fig. 1a) proposed in Ref. [3] is nonexistent since neither the XRD nor the DSC data provide any evidence for its existence.

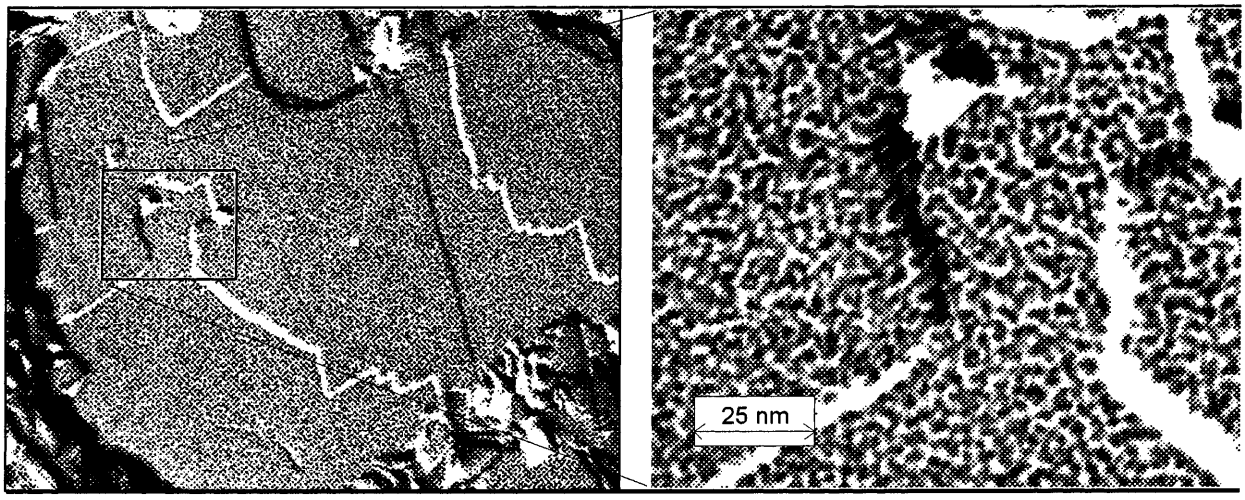

Fig. 11 TEM image of a freeze-fracture representation of a sample containing KC_{14}/Gl, $x_{KC_{14}} = 0.37$, at $T = 403$ K within the L_α phase region of the phase diagram

A comparison of the d values of the first small-angle reflexes with the DSC curve obtained for rising and falling temperatures is shown in Fig. 12. The C ↔ G phase transition is accompanied by the characteristic splitting of the first small-angle reflex and a correlated sharp shift of the d value of $\Delta d \approx +0.25$ nm. The DSC curve for cooling shows that the phase transitions can be undercooled by about $\Delta T \approx 10$ K.

Investigations of the KC_{14}/Gl system with a concentration $x_{KC_{14}} = 0.50$

According to Fig. 1 the phase sequence C ↔ G ↔ L_α was expected at this concentration for rising temperatures. The wide-angle diffractograms and the DSC curve for rising temperature are displayed in Fig. 13. Comparing the diffractograms one finds that during the C ↔ G phase transition the distinct strong three reflexes at $2\Theta \approx 18.7°$, 23.6°, and 21° disappear. The remaining reflexes are rearranged and reduced in intensity. Furthermore, a peculiar broad reflex appears at $2\Theta \approx 27°$. Also, the elevated wide-angle background is intensified due to the increased amorphous portions of the structure. The G ↔ L_α transition occurs over a temperature range of $\Delta T \approx 20$ K and is therefore comparatively broad.

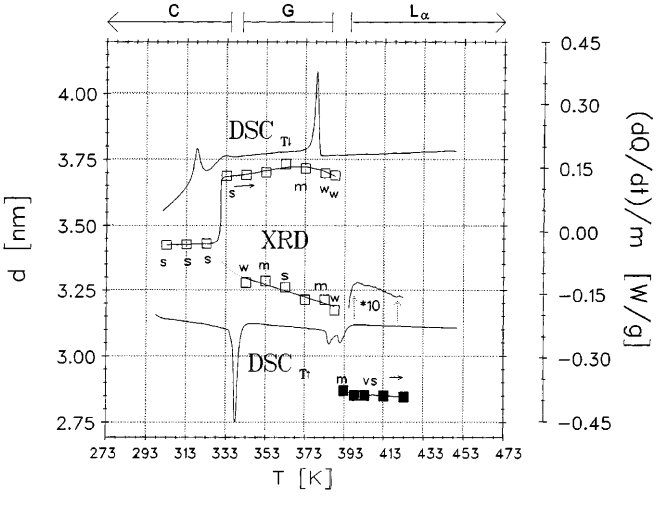

Fig. 12 Comparison of the d values of the first small-angle reflexes with the DSC curve obtained for rising and falling temperatures of the KC_{14}/Gl system, $x_{KC_{14}} = 0.37$. □ reflexes of the C and G phases, ■ reflexes of the L_α phase

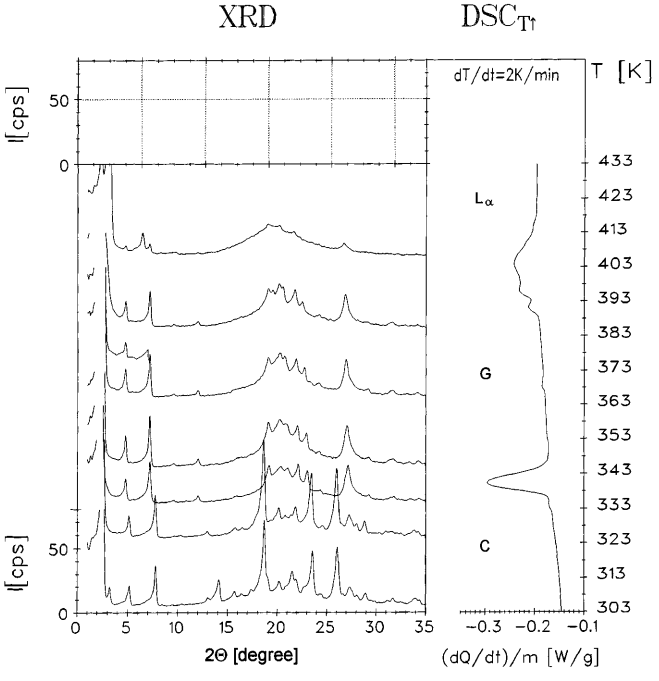

Fig. 13 Comparison of wide-angle X-ray diffractograms with the DSC curve for rising temperature of the KC_{14}/Gl system, $x_{KC_{14}} = 0.50$

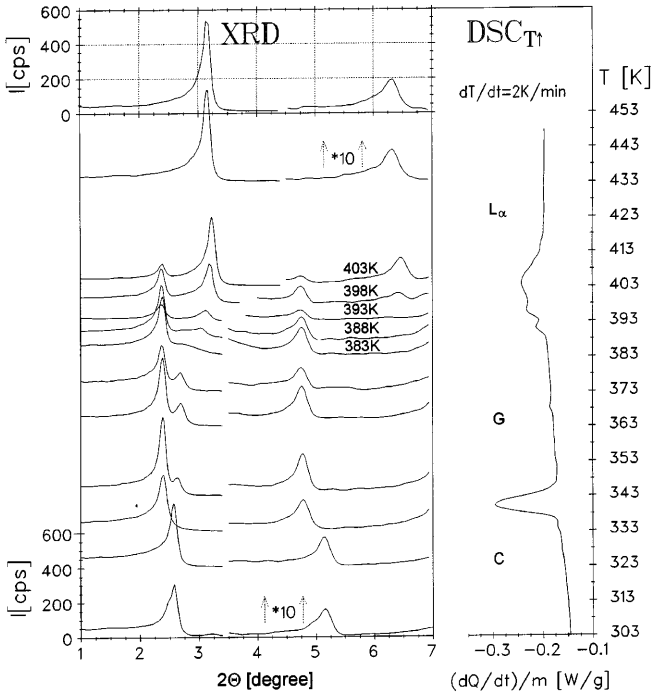

Fig. 14 Comparison of small-angle X-ray diffractograms with the DSC curve for rising temperature of the KC_{14}/Gl system, $x_{KC_{14}} = 0.50$

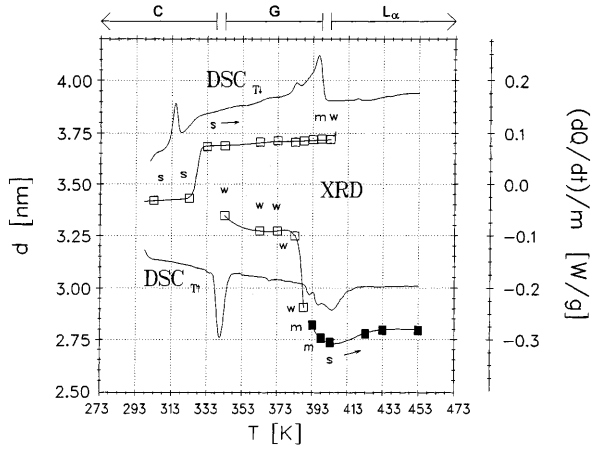

Fig. 15 Comparison of the d values of the first small-angle reflexes with the DSC curve obtained for rising and falling temperatures of the KC_{14}/Gl system, $x_{KC_{14}} = 0.50$. □ reflexes of the C and G phases, ■ reflexes of the L_α phase

The small-angle diffractograms and the DSC curve for rising temperature are compared in Fig. 14. The broad $G \leftrightarrow L_\alpha$ phase transition can be traced very clearly in the diffractograms. The first reflex at $2\Theta \approx 2.38°$ gradually loses intensity between $T = 343$ and 383 K while at the same time the second reflex at $2\Theta \approx 2.70°$ constantly increases in intensity. The corresponding d values and the DSC curve obtained for rising and falling temperatures are summarized in Fig. 15. Again it is observed that the $C \leftrightarrow G$ phase transition correlates with a splitting of the first of the small-angle reflexes and an equivalent shift of $\Delta d \approx +0.25$ nm. The $G \leftrightarrow L_\alpha$ phase transition is preceded by a sharp decrease in the d value of $\Delta d \approx -0.35$ nm between $T = 383$ and 388 K. During the initial stages of the L_α phase the d values again reach a minimum falling to $d = 2.72$ nm and remain constant at $d = 2.79$ nm for higher temperatures within the measured range.

Conclusions

According to the phase diagram shown in Fig. 1b, the following phases exist in the KC_{14}/Gl binary system: the C phase, the L_α phase, the H_α phase, the G phase and the isotropic, micellar solution S. Analogously to the KC_{12}/Gl binary system discussed in Ref. [2], the separating line between the H_α and S phases has a maximum.

All the XRD and DSC measurements as well as the electron microscopic investigation have undoubtedly proven that a correction of the preliminary phase diagram from Ref. [3] is necessary with respect to the so called G_1 phase and the I phase. Actually, both phases do not exist: neither the second G phase nor the I phase could be confirmed by the XRD and DSC measurements. The correct phase diagram is shown in Fig. 1b, wherein both phases no longer appear, while the region of the L_α phase is extended. Consequently, in the range of low KC_{14} concentrations $x_{KC_{14}} \lesssim 0.26$ a $C \leftrightarrow H_\alpha \leftrightarrow S$ polymorphism exists. For concentrations $x_{KC_{14}} > 0.30$ the polymorphous $C \leftrightarrow G \leftrightarrow L_\alpha$ transitions occur.

Interestingly, our results are similar to those of investigations of liquid crystalline structures of cationic surfactants in nonaqueous solvents [5–7]. In these nonaqueous systems the authors measured lamellar distances of the same order of magnitude by XRD.

References

1. Hieke A, Dörfler HD Colloid Polym Sci
2. Hieke A, Dörfler HD Colloid Polym Sci
3. Dörfler HD, Senst A (1993) Colloid Polym Sci 271:173–189
4. Hieke A (1995) Thesis. TU Dresden
5. Dékány I, Szántó F, Weiss A, Lagaly G (1986) Ber Bunsenges Phys Chem 90:422–427
6. Dékány I, Szántó F, Weiss A, Lagaly G (1986) Ber Bunsenges Phys Chem 90:427–431
7. Dékány I, Szántó F, Weiss A (1989) Colloids Surf A 41:107–121